

**IV. CONSTRUCTION, WIND TUNNEL TESTING
AND DATA ANALYSIS FOR A 1/5 SCALE
ULTRA-LIGHT WING MODEL**

Michael D. James
Graduate Student

Howard W. Smith
Professor
Department of Aerospace Engineering
University of Kansas

December 1988

Partially supported by
NASA Langley Research Center
Grant #NAG 1-345

SUMMARY

This report documents the construction, wind tunnel testing and the data analysis of a 1/5 scale ultra-light wing section. The original ultra-light this wing model is scaled after is Dr. Howard W. Smith's structural test ultra-light located at the Lawrence airport.

Wind tunnel testing provided accurate and meaningful lift, drag and pitching moment data. This data was processed and graphically presented as:

C vs. α
L

C vs. α
D

C vs. α
M

C vs. C
L D

The wing fabric flexure was found to be significant and its possible effects on aerodynamic data was discussed. The fabric flexure is directly related to wing angle of attack and airspeed. Different wing section shapes created by fabric flexure are presented with explanations of the types of pressures acting on the wing surface.

This report provides conclusive aerodynamic data about ultra-light wing. This topic is well worthwhile for continuing studies.

TABLE OF CONTENTS

<u>Item</u>	<u>Page</u>
1. Introduction	1
2. Wing Construction	2
3. Wind Tunnel Testing Method	7
4. Test Trials	10
5. Data Analysis	12
6. Wing Fabric Flexure	18
7. Recommendations and Conclusions	24
Appendix A: Data Analysis	A

1. INTRODUCTION

This special project was performed to study the basic aerodynamic characteristics of an ultra-light wing. Few known wind tunnel tests have been performed of ultra-light wings since they are designed to be very inexpensive. Thus, aerodynamic data such as the variation angle of attack with lift coefficient, drag coefficient, or pitching moment coefficient is relatively unknown. Another specialty about ultra-light wings is that aerodynamic data becomes a function of wing fabric flexure, which itself is function of airspeed and angle of attack.

To perform these wind tunnel tests, a one-fifth scale wing model of Howard Smith's experimental test ultra-light was constructed. Particular attention was paid to keeping the wing model true-to-scale so that hopefully scale aerodynamic characteristics could be studied.

This wing was sized to fit in the small subsonic wind tunnel in the basement of Learned Hall. The two column support rod was used for the test mount. the aerodynamic forces were read by a balance table and displayed on a scale. This data was processed and displayed as standard C_l , C_d and C_m vs. α data.

2. WING CONSTRUCTION

The wing construction consisted of five phases:

- 1) scaling the wing
- 2) plotting the airfoil coordinates
- 3) sizing the wing
- 4) selecting materials
- 5) construction

Phase 1. Scaling the wing

The wing was primarily scaled down by measuring the chord and thickness of Dr. Smith's test ultra-light wing at the Lawrence airport and applying various scales to determine sizing. Scales of 1:10, 1:5 and 1:4 were considered. The scale of 1:5 was selected since it would size a model with a maximum thickness of 1.3 inches and chord of 10.2 inches; ideal size for the small subsonic wind tunnel.

Phase 2. Plotting the airfoil coordinates:

In order to perform this step, I visited the Lawrence airport where Dr. Smith's ultra-light is currently hoisted and being prepared for structural testing. To plot the airfoil coordinates, two methods were used:

- 1) plotting points measured on the wing surface
- 2) plotting points measured inside the wing

By plotting both sets of coordinates, erroneous data points could be eliminated and the airfoil surface could be developed. An airfoil section is shown in Figure 2.1. Note the flat bottom of the airfoil and the constant slope in the upper camber between half chord and the trailing edge. Figure 2.1 also shows the location and attitude of the mounting block in the wing. The mounting block is situated so that an angle of attack range of +20 to -10 degrees can be achieved.

Phase 3. Sizing the wing:

The wing was sized to create approximately 25 pounds of lift at maximum angle of attack at an airspeed of 75 feet per second. A maximum lift coefficient of 1.6 was assumed. It was figured that a wing area of 2.3 square feet was needed. The wing span was incremented by a scale rib spacing until the size was either 2.3 square feet or until the span was too large for the tunnel. A wing with four rib spacings was calculated to have an area of 2.0 square feet and a span of 2.35 feet. Perfect! the area requirement is close and it fits in the tunnel (with an inch on each wing tip to spare).

Phase 4. Selecting materials:

Since "scale" materials were too hard to find and were usually too expensive or hard to work with, substitute materials were used. A list of the materials and their uses is:

<u>Material</u>	<u>Size</u>	<u>Purpose</u>
1) Birch dowels	3/8" 1/2"	front spar (leading edge) rear spar
2) Birch plywood	3/32" 5-ply	wing ribs
3) Oak block	1" thick	mounting attachment
4) Music wire	1/32" 1/16	trailing edge stiffeners lower surface fabric supports, wing chord trailing edge supports
5) Nylon fabric	---	wing fabric
6) Two ton epoxy	---	used for wood-metal bonds
7) Wood glue	---	used for wood-wood and wood-fabric bonds

Phase 5. Construction:

Construction started by preparing the the wing ribs. First the plywood sheet was cut, mounted together and bonded lightly. Wing rib templates were laid out and holes for the front spar and rear spar were drilled. Next the wing ribs were cut out by a ban saw which insured that each rib would be the same size and shape. They were separated, sanded and bonded together in pairs. A 2.5 inch section of music wire was epoxied into a groove cut in to the trailing edge to simulate the trailing edge shape of the airfoil. The wing ribs were glued onto the front and rear spars maintaining a 1/5 scale distance between each wing rib and a 1 inch spacing between the two center ribs for mounting block.

Once the main wing structure was bonded together, the trailing edge music wire was added. The music wire in the model performs the function of the cables in the ultra-light. The music wire was soldered and glued to the trailing edge of the plywood wing ribs and the music wire extensions. Solder and epoxy lumps were files out to keep the trailing edge to a minimum thickness. 1/16" music wire supports were added in a criss-cross fashion between the leading edge and the main spar of the wing lower surface. These act as cables do in the ultra-light to provide fabric support. At this point, before the covering, the mounting

block was glued into place. Figure 2.2 shows two photographs of the uncovered wing frame.

The wing was finally covered with the nylon fabric. Wood glue was used since it binds between the fabric filaments. The fabric covering was stretched tight in the gluing process simulating that of the ultra light. An abundance of glue was used to provide a good rib-fabric bond since the fabric must carry the entire wing loading.

Overall, the model is an excellent 1/5 scale representative of the full size ultra-light wing.

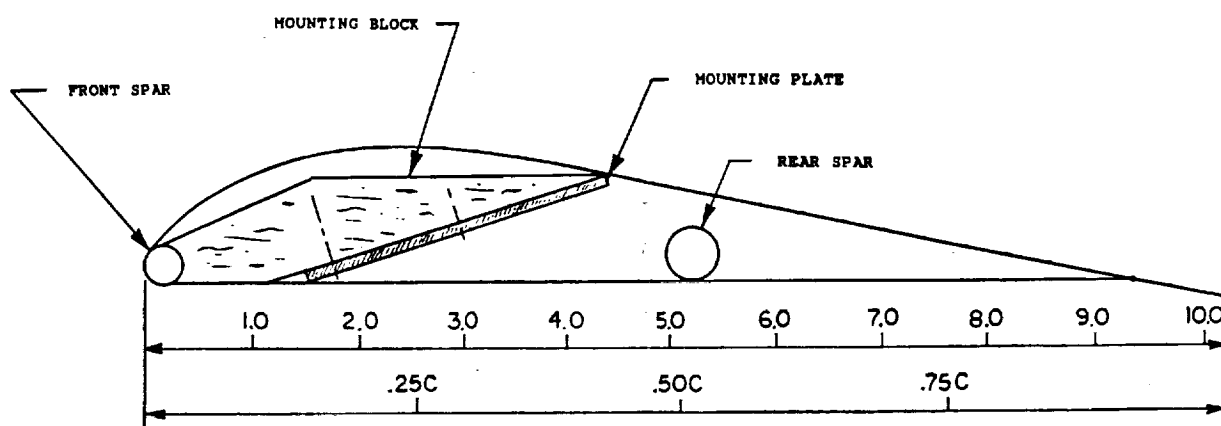


FIGURE 2.1 WING CROSS SECTION

C-2

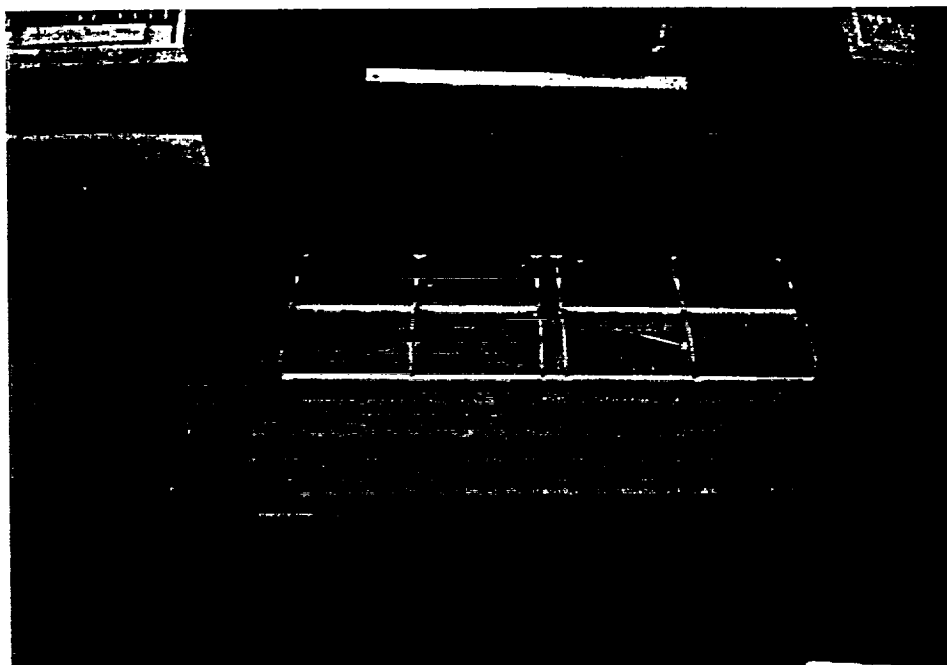


FIGURE 2.2 UNCOVERED WING FRAME

3. WIND TUNNEL TESTING METHOD

Once construction of the 1/5 scale ultra-light wing was finished, the wing was mounted in the small subsonic wind tunnel in the basement of Learned hall. Figure 3.1 shows a 3/4 view of the wing in the test section. Figure 3.2 shows a front view of the wing in the test section from inside the wind tunnel.

Raw data from the tunnel testing appears in Appendix A. The following data is included in the upper portion of these data sheets:

* Wind tunnel static pressure: P_s

* Wind tunnel total pressure: P_T

* Ambient temperature

* Atmospheric pressure

Once the tunnel is up to testing velocity lift, drag, and pitching moment were read off of a percent of range scale and recorded for a range of attack angles. The wing angle of attack is varied during the test run.

The basic purpose of the testing was to determine the aerodynamic data of the wing and compare it with regular airfoil data. During the testing it became apparent that the airfoil section shape, and thus aerodynamic data, depends highly on the fabric flexure. The fabric flexure is in turn determined by the airspeed and angle of attack of the wing. These compounding factors cannot be completely assessed individually but they are considered in explaining the aerodynamic data. Wing sections will be shown at varying angles of attack.

Eight individual tunnel test runs were performed for the ultra-light wing model. Tunnel speeds range in between 47 and 121 feet per second. Extreme caution was used in making certain that the wing would not receive loadings large enough to cause structural failure. This model is not designed to sustain lift or drag loadings over thirty pounds because of its light construction. This limit maximum limit loading on the model wing is, by the way, equivalent to fifteen pounds per square foot--the loading normally sustained by light all metal aircraft!

The aerodynamic forces carried through the wing are sensed by a force table beneath the test section of the wind tunnel. Strain gauges in the force table translate lift drag and pitching moment forces into electrical voltages through a Wheatstone bridge circuit. The data is finally displayed on a control panel which has selector knobs for lift, drag, pitching moment and scale factor and a percent of range scale for voltage reading. The scale factor knob

has magnitude selections of 50, 100, 200, 500, 1000 and 2000. The scale factor is read in percent of range which varies between $-.5$ and $+.5$. The scale factor and voltage are read for lift, drag and pitching moment for each angle of attack tested per trial.

Test runs #1 and #2 are considered inconclusive evidence. It was discovered through these tests that varying the scale factor caused significant error because only one scale factor can be zeroed to at a time. For the remaining tests the percent of range scale was zeroed to a certain scale factor, which was used for the entire test.

ORIGINAL PAGE
BLACK AND WHITE PHOTOGRAPH

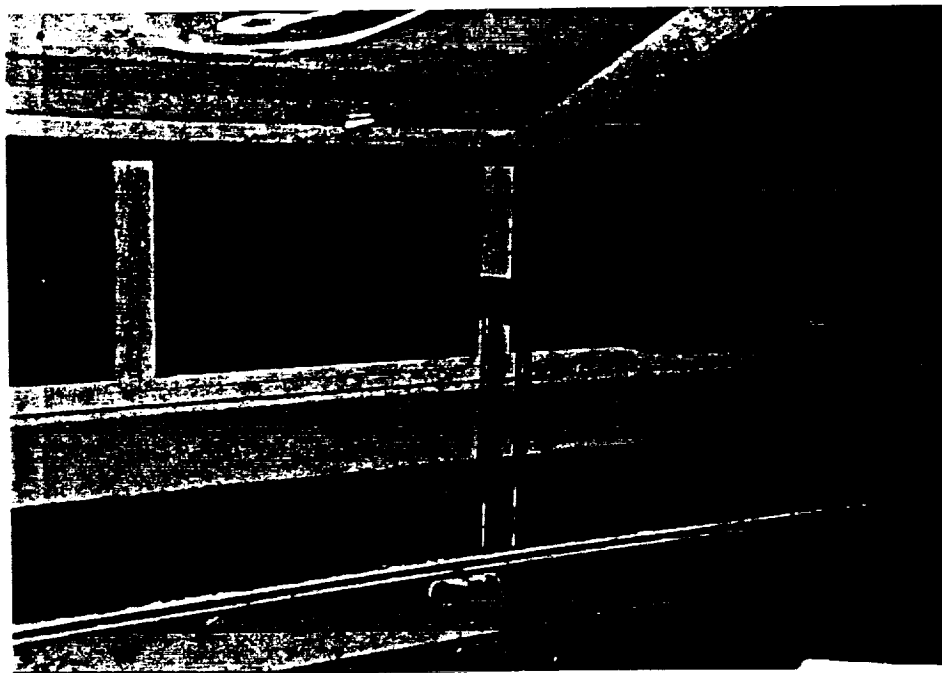


FIGURE 3.1 WING MOUNTED IN THE TEST SECTION:
3/4 VIEW

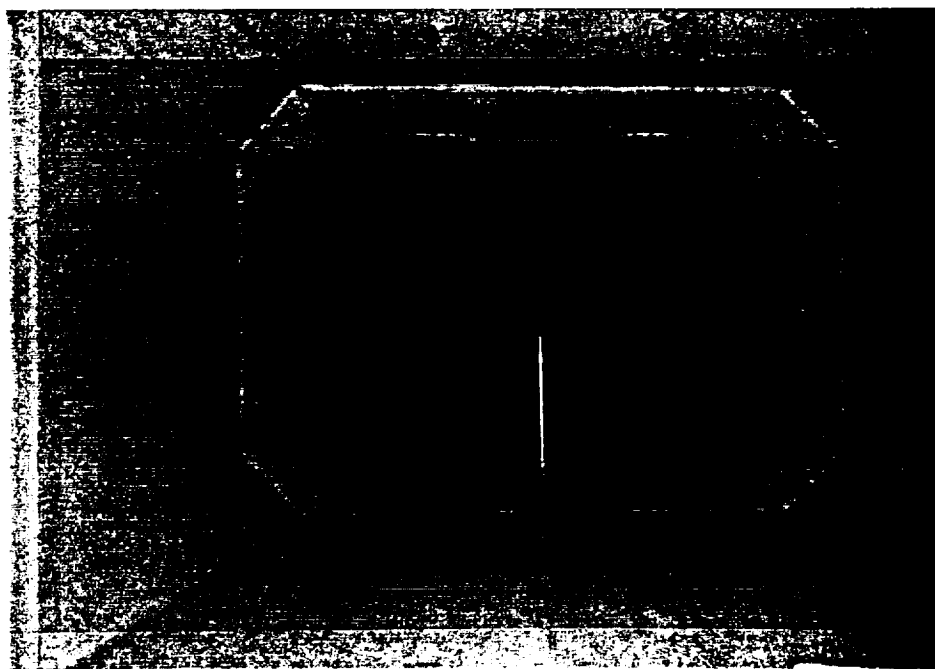


FIGURE 3.2 WING MOUNTED IN THE WIND TUNNEL
FRONT VIEW

ORIGINAL PAGE
BLACK AND WHITE PHOTOGRAPH

4. TEST TRIALS

Eight different testing runs were recorded. Trial numbers 1 and 2 are inconclusive but served to demonstrate a more accurate method of testing; picking one scale factor and using it for the entire test run. The remaining tests all provide meaningful data. These tests were run at different wind tunnel velocities, which were selected as to maintain a useful range of data.

Test #3: The scale factor of this particular test was set at 2000. The tunnel velocity was incremented until the maximum drag reading (at 20 degrees angle of attack) read the maximum of .5 on the scale. The wing angle of attack was varied from +20 degrees to -12 degrees by increments of 2 degrees. Lift and drag data was recorded for this trial. Noted are that buffeting occurred at -12 degrees and beyond +8 degrees. This was seen to be the case for the remaining trials.

Test #4: This test was run to obtain a complete record of lift, drag and pitching moment data. With the scale factor set at 2000, the tunnel velocity was stabilized so that the maximum pitching moment reading was -.5. This tunnel velocity is the maximum limit for complete lift drag and pitching moment data. This also means that the wing is oversized: the aerodynamic forces that the wing capable of are larger than those that can be supported by the balance table. This test was performed for an angle of attack range of +20 degrees to -12 degrees.

Test #5: This test is the first 'high speed' trial of the wing model. 'High speed' for this model is considered to be greater than 100 feet per second, which is the approximate tunnel velocity of this trial. The angle of attack range selected is +12 to -12 degrees. Again, structural constraints limited the maximum wing angle of attack. Lift and drag data only were recorded.

Test #6: This test is the second 'high speed' trial. This test is very similar to test #5 except a larger wind tunnel velocity was used; approximately 122 feet per second. This is the maximum recommended tunnel velocity to be used for this wing. Because of the high speed, the variation of angle of attack was maintained between +8 and -8 degrees. The main purpose of this test is to compare the lift and drag data of high speed trials to lower speed trials.

Test #7: This test is a duplication of test #4. The same approximate tunnel speeds were used and the same angle of attack range was used. The purpose of this test is to determine the the test replicability of this testing procedure by attempting to duplicate the results.

Test #8: This test is the 'low speed' trial. The scale factor used for this test was 1000. Again, the pitching moment reading was the limiting factor: the tunnel velocity was set such that the maximum pitching moment registered -.5 on the percent of scale range. Angle of attack for this trial was varied between 20 and -12 degrees.

5. DATA ANALYSIS

Of the eight wind tunnel test runs performed, six trials had meaningful data. These data for these six wind tunnel tests was processed and they are displayed in this chapter in the following figures:

- Figure 5.1: Section Lift Characteristics for the 1/5 Scale Ultra-Light Wing Model
- Figure 5.2: Section Drag Characteristics for the 1/5 Scale Ultra-Light Wing Model
- Figure 5.3: Section Pitching Moment Characteristics for the 1/5 Scale Ultra-Light Wing Model
- Figure 5.4: Drag Polar Characteristics for the 1/5 Scale Ultra-Light Wing Model

The raw wind tunnel data is listed in Appendix A. The equations which relate percent of range and scale factor readings into actual lift, drag and pitching moment forces were obtained from an AE 245 laboratory exercise. These equations and along with lift, drag and pitching moment equations were written into a basic program to speed up the data analysis program. The final output of this program gives the tunnel speed, Reynold's number and the wing lift coefficient, drag coefficient and pitching moment coefficient. The output listing for runs 3-8 are in Appendix A.

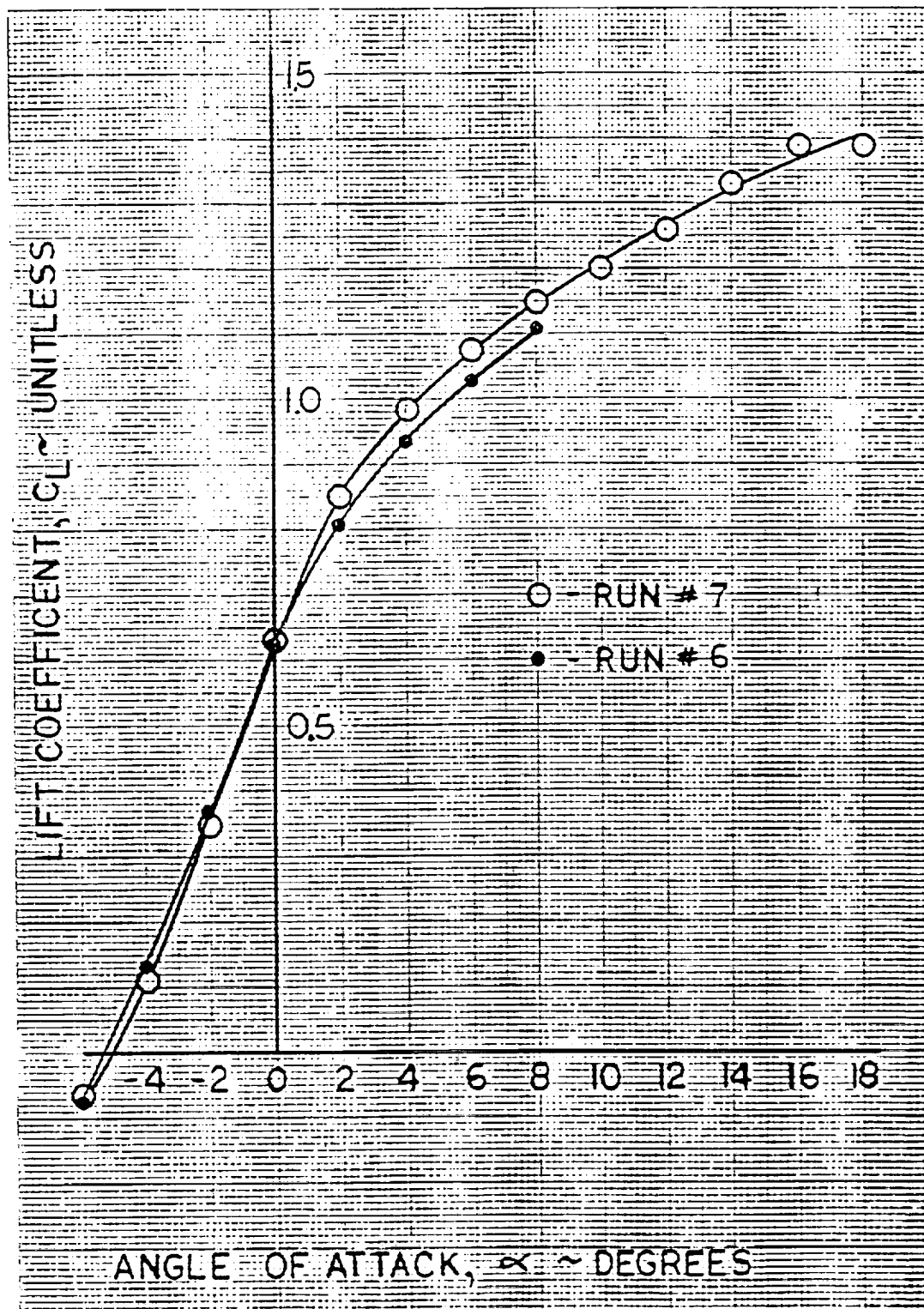
The lift coefficient-angle of attack curve is seen in Figure 5.1. Data from trials number 6 and 7 were plotted. Although these two trials were performed at 122 and 67 feet per second respectively, the data compares very well. The lift coefficients at higher angles of attack for the high speed case lies below those for the low speed case. This most likely indicates that wing section deformation at higher speeds lowers the wing's lift producing efficiency. An unusual characteristic of this lift curve is that there appears to be two different and distinct lift curve slopes. Between -4 and +2 degrees angle of attack the lift curve slope is roughly 7.6 per radian. Between +6 and 16 degrees angle of attack the lift curve slope drastically drops to 1.8 per radian. This indicates that this wing section does not generate much incremental lift coefficient at high angles of attack. Also evident is that lift coefficient is very sensitive to angle of attack change at small angles of attack. Another interesting characteristic of this wing section is the high lift at zero angle of attack. The angle of zero lift is approximately -5 degrees. Obviously this wing section generates a relatively large margin of positive lift at small negative angles of attack.

The drag coefficient-angle of attack curve is seen in Figure 5.2. Data for this plot was taken from test run #3. Minimum drag for this wing section occurs between -4 and -2 degrees angle of attack. It should be clarified that this drag is for the entire model and support mount! No tare

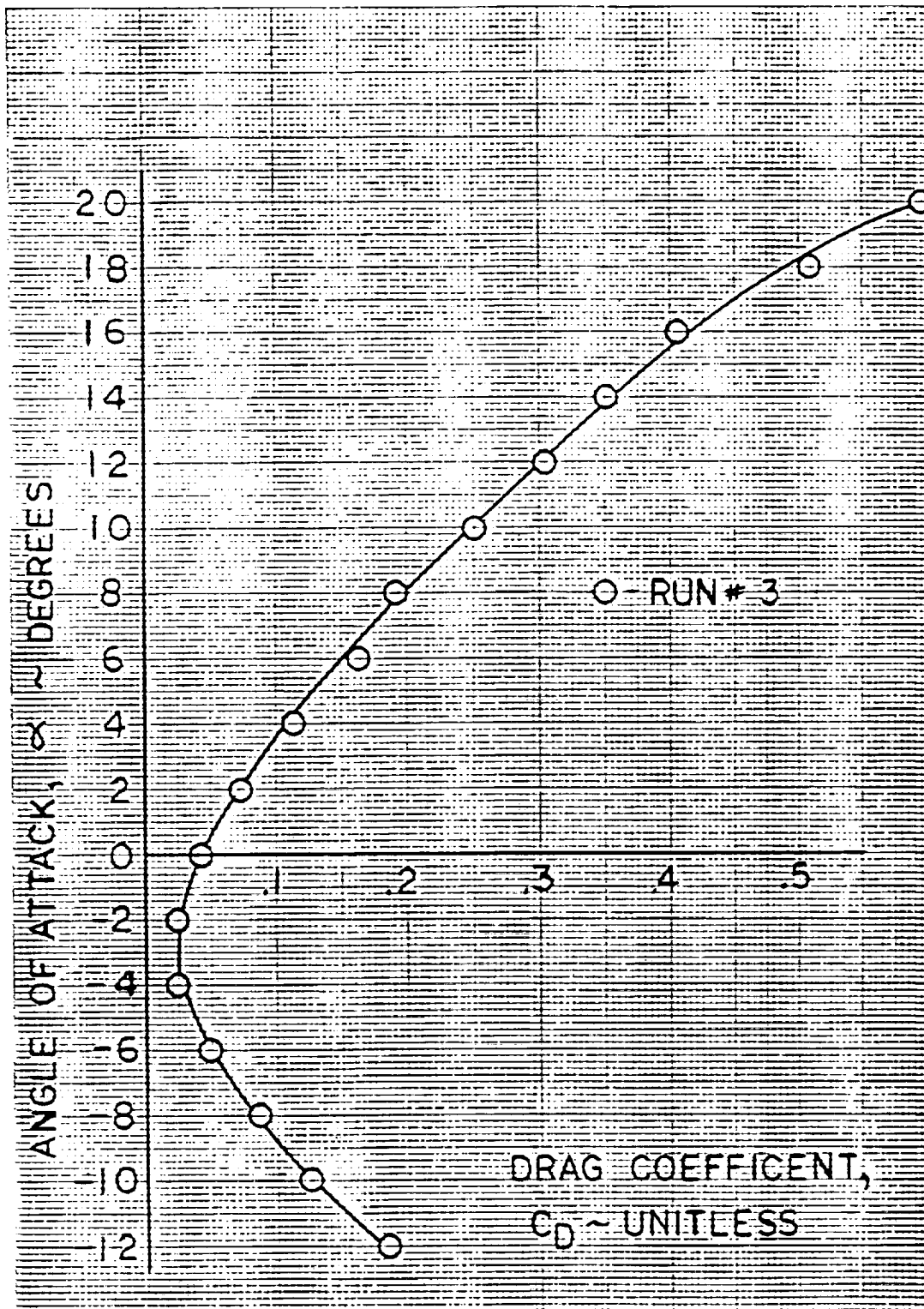
runs were performed due to time restrictions. Since most of the data runs were taken at low speeds and since the model is relatively large this won't create a significant error. The drag bucket in this curve also seems fairly symmetrical between -12 and +8 degrees angle of attack. One interesting characteristic of this curve is the intense amplification of drag at large angles of attack. The drag reading at 20 degrees is a factor of 24 times larger than the drag reading at -2 degrees. This "amplification factor" in ordinary wings is usually not as large. This is perhaps caused by the wing fabric pocketing at high angles of attack and further destroying the air flow. Another possible theory is derived from the fact that the wing frontal area to tunnel test section area ratio is small at large angles of attack. The airflow is constrained to this area, and normal flow probably cannot be achieved, and the air pressure is probably increased, thus the drag is increased. A third possibility of excess drag at high angles of attack could be due to the model flutter at these angles. The model was seen to flutter at -12 degrees and above +8 degrees angle of attack. Drag is known to increase with flutter.

The pitching moment-angle of attack curve is seen in Figure 5.3. Data for this plot was taken from test run #7. It should be reminded that this pitching moment data is about the main model support mount which is located at .18c of the wing. Pitching moment data is usually referenced at .25c or the aerodynamic center. A simple transformation can be performed to shift the pitching moment coefficient to this point but time constraints limited this process. Nevertheless, the slope and shape of the pitching moment curve is accurate and can be commented on. The slope of a pitching moment-angle of attack curve should ideally be a straight line. The pitching moment curve plotted indicates three different upwardly sloping "troughs". The angle of attack breaks between the three troughs are 0 degrees and 14 degrees. It is uncertain what causes these distinct breaks, but again it is assumed to be the fabric flexure. Apparently fabric flexure change at 0 and 14 degrees angle of attack is very critical to pitching moment characteristics of the wing.

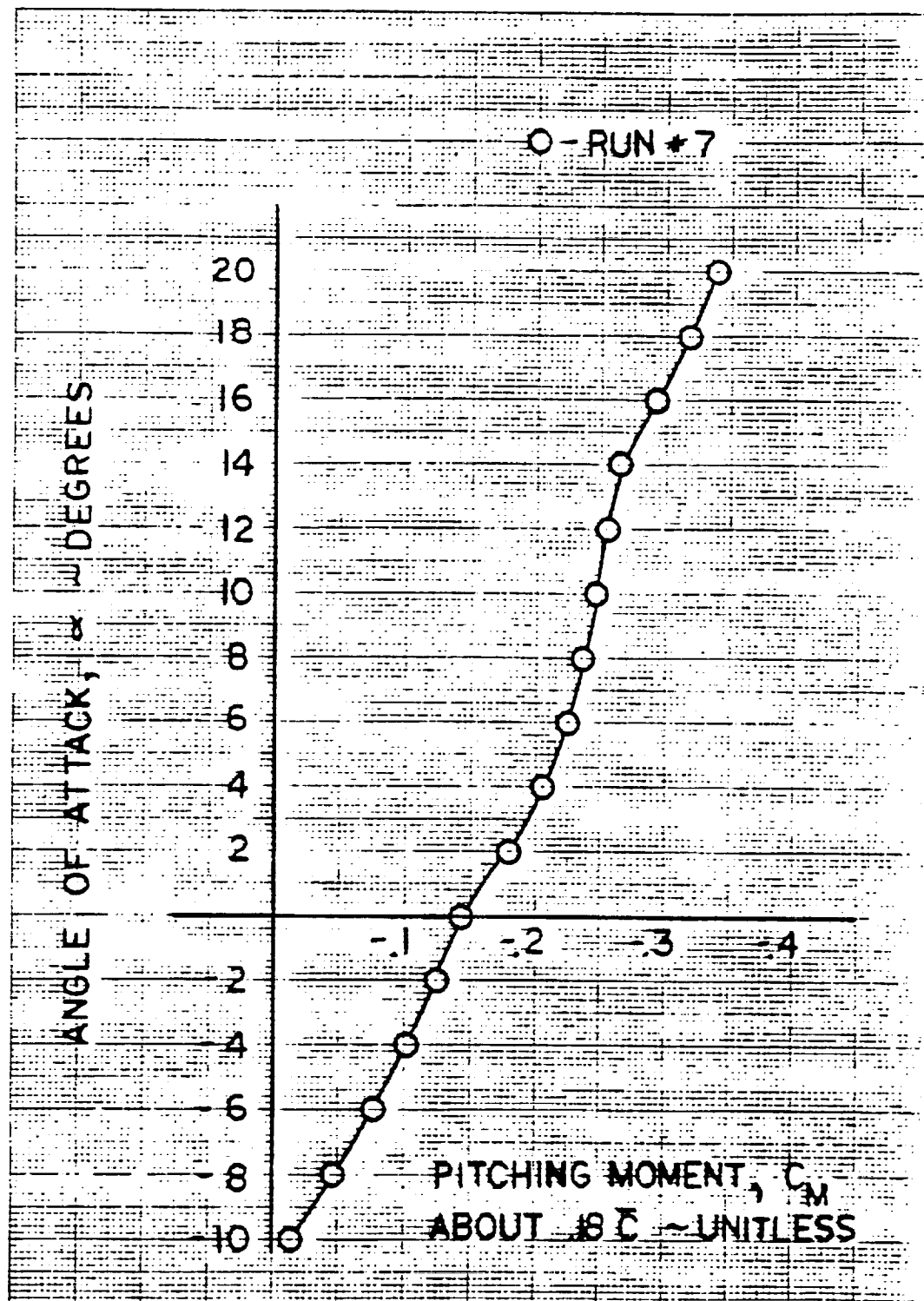
The lift coefficient-drag coefficient curve is seen in Figure 5.4. Data for the two curves were taken from test runs #6 and #8, the high speed and low speed trials, respectively. The slope of this curve indicates the maximum lift to drag ratio of the model. For the low speed case (run #8) the maximum lift to drag ratio is 12. The maximum lift to drag ratio for the high speed case (run #6) is 7. This indicates that the lift to drag ratio is reduced at higher speeds. This is probably because the fabric flexure at higher speeds is more warped and less conducive to lift.



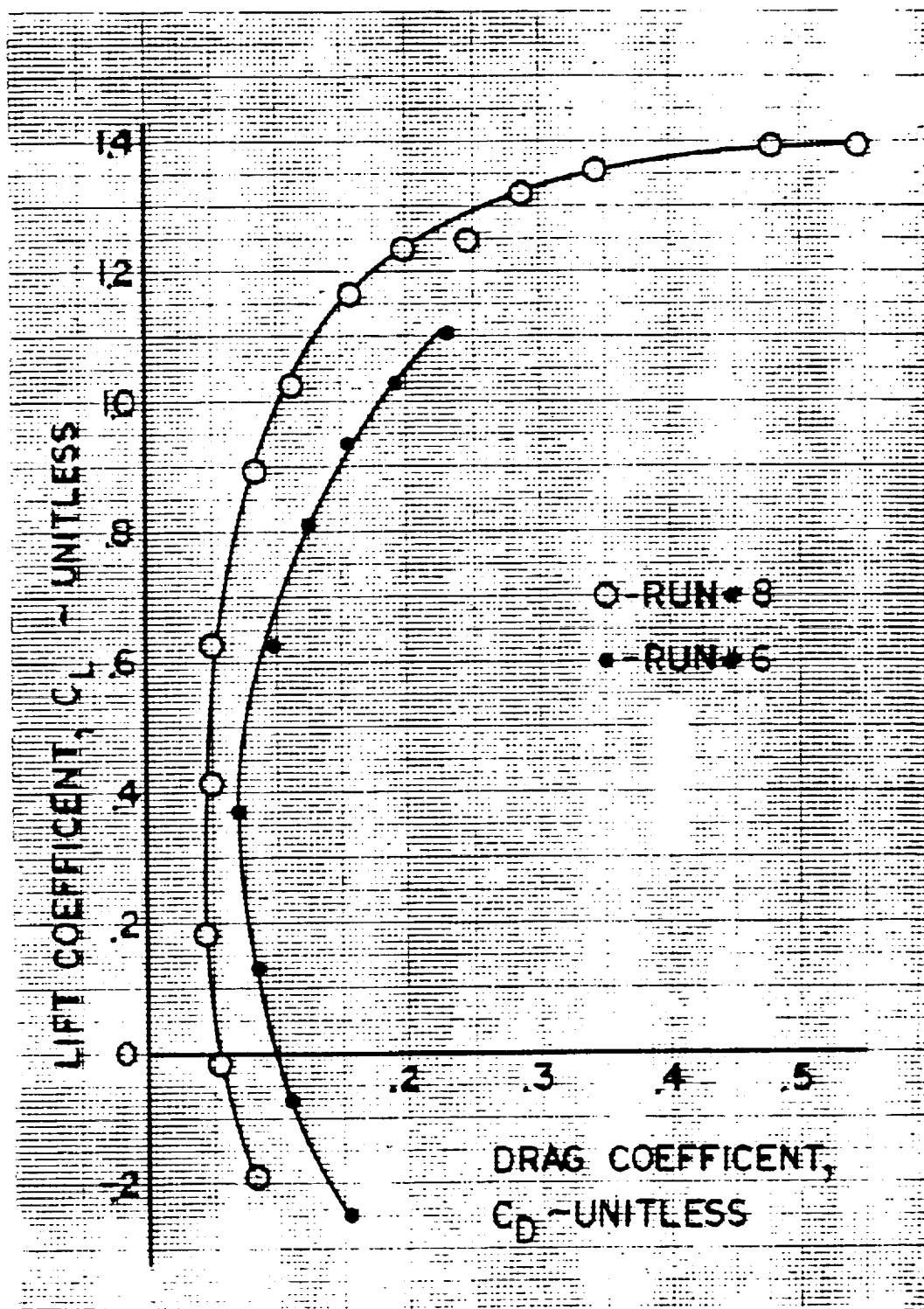
CALC	M. James		REVISED	DATE	FIGURE 5.1 SECTION LIFT CHARACTERISTICS FOR THE 1/5 SCALE ULTRA-LIGHT WING MODEL	AE 592
CHECK						
APPD						
APPD						
					UNIVERSITY OF KANSAS	PAGE 14



CALC	M. James		REVISED	DATE	FIGURE 5.2 SECTION DRAG CHARACTERISTICS FOR THE 1/5 SCALE ULTRA-LIGHT WING MODEL	AE 592
CHECK						
APPD						
APPD						
					UNIVERSITY OF KANSAS	PAGE 15



CALC	M. James		REVISED	DATE	FIGURE 5.3 SECTION PITCHING MOMENT CHARACTERISTICS FOR THE 1/5 SCALE ULTRA-LIGHT WING MODEL	AE 592
CHECK						
APPD						
APPD						
					UNIVERSITY OF KANSAS	PAGE 16



CALC	M. James		REVISED	DATE	FIGURE 5.4 DRAG POLAR CHARACTERISTICS FOR THE 1/5 SCALE ULTRA-LIGHT WING MODEL	AE 592
CHECK						
APPD						
APPD						
					UNIVERSITY OF KANSAS	PAGE 17

6. WING FABRIC FLEXURE

The topic of wing fabric flexure was mentioned often in the previous chapter. The section shape of an ultra-light wing is highly variant to airspeed and angle of attack. Airspeed tends to vary the magnitude of the fabric flexure. Angle of attack varies the location and direction (inwards or outwards) of fabric flexure. The fabric flexure for five different angle of attack settings were sketched in Figures 6.1 to 6.5. The many different (and odd !) airfoil shapes should be noticed for the range of attack angle settings. These figures show generalized airfoil shapes. The wing model was constructed with wire cross braces on the lower surface between the leading edge and main spar for fabric support (as stated in the construction chapter) which obviously are reflected in the lower surface fabric flexure shape. These helped to limit the fabric deflection in that particular area, but the exact shape they create is not determined in the figures.

-10 degrees angle of attack: This setting is shown in Figure 6.1. The upper surface leading edge and trailing edge are indented signifying a pressure force exerted downward on the wing. The entire lower surface is bubbled outwards, again displaying a downwards pressure force. There is a very interesting bubble in the fabric on the upper surface of the wing at about .25c. This perhaps is the only upwards pressure force on the wing, and serves to form a very unusual airfoil surface.

-6 degrees angle of attack: This setting is shown in Figure 6.2. The upper surface leading edge and trailing edge are indented, and so is the lower surface trailing edge. These indented surfaces are all handling inward pressure forces. The surfaces bubbling outward (experiencing outward pressure forces) lie on the middle upper surface and the lower leading surface of the wing.

0 degrees angle of attack: This setting is shown in Figure 6.3. The upper surface leading edge and entire lower surface of the wing are experiencing inward pressure forces. The remaining upper surface is bubbled outward and is experiencing lift.

6 degrees angle of attack: This setting is shown in Figure 6.4. It is virtually identical to the setting of zero degrees in Figure X.4. The only difference is that the upper surface fabric bubbling is more marked.

20 degrees angle of attack: This setting is shown in Figure 6.5. This is quite similar to the previous two settings (0 and 6 degrees), however the upper surface leading edge and lower surface fabric deflection is more marked, and the upper surface bubble is shifted more aft.

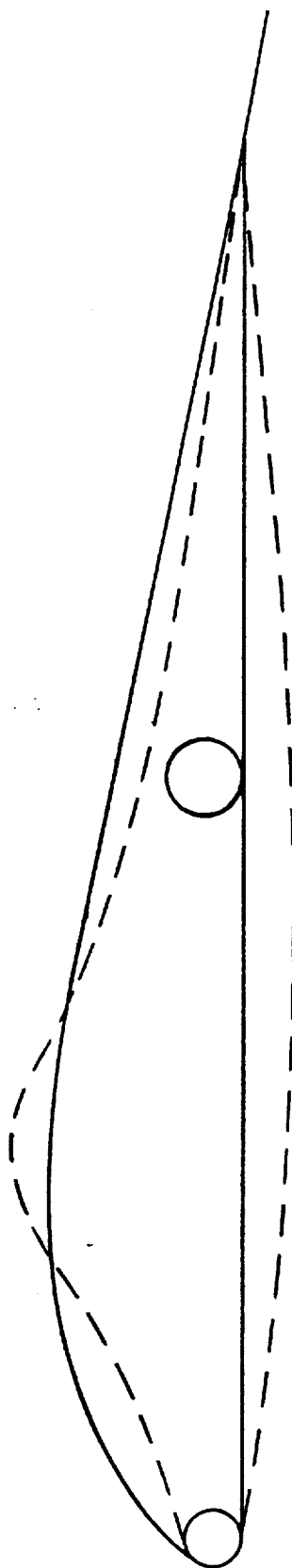


FIGURE 6.1 WING SECTION SHAPE DUE TO FABRIC FLEXURE
AT -10 DEGREES ANGLE OF ATTACK

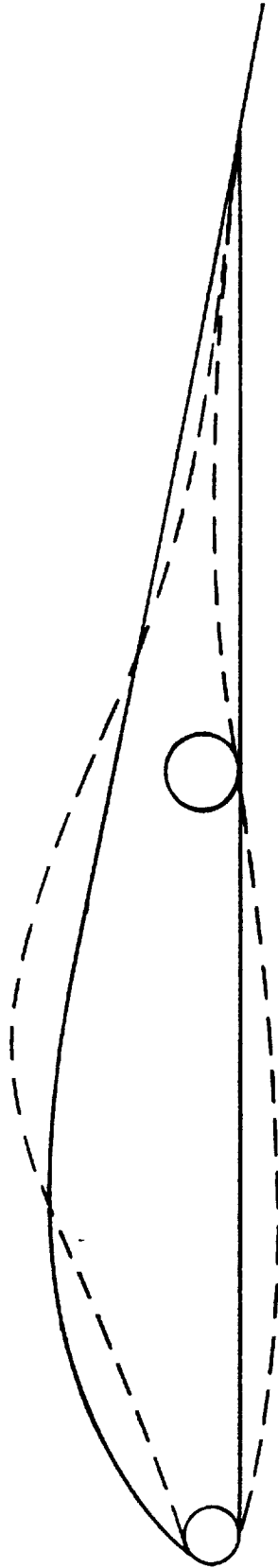


FIGURE 6.2 WING SECTION SHAPE DUE TO FABRIC FLEXURE
AT -6 DEGREES ANGLE OF ATTACK

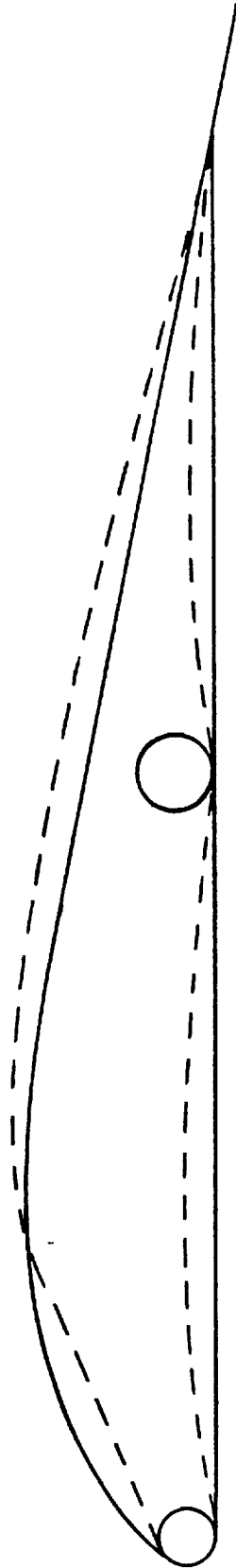


FIGURE 6.3 WING SECTION SHAPE DUE TO FABRIC FLEXURE
AT 0 DEGREES ANGLE OF ATTACK

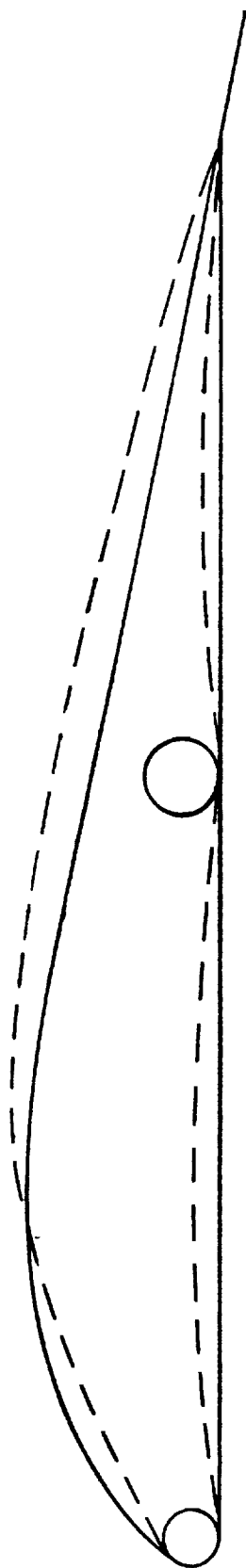


FIGURE 6.4 WING SECTION SHAPE DUE TO FABRIC FLEXURE
AT +6 DEGREES ANGLE OF ATTACK

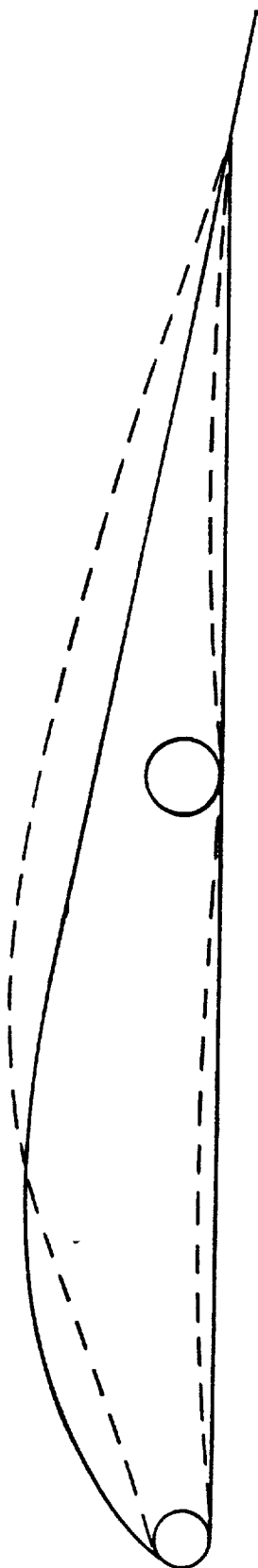


FIGURE 6.5 WING SECTION SHAPE DUE TO FABRIC FLEXURE
AT +20 DEGREES ANGLE OF ATTACK

7. RECOMMENDATIONS AND CONCLUSIONS

This project is an initial attempt to provide aerodynamic data for an ultra-light wing. Conclusive and fairly accurate lift, drag and pitching moment data were recorded and analyzed for the wing model. Some of the important findings are:

- 1) The lift coefficient-angle of attack curve indicated the presence of two entirely different lift curve slopes at different angles of attack.
- 2) The change in drag between small and large angles of attack is quite marked.
- 3) There occur two distinct break points on the pitching moment coefficient-angle of attack curve, indicating a particular sensitivity at these two angles of attack.
- 4) Lift to drag ratios for this model are 12 at low speeds and 7 at high speeds.
- 5) Aerodynamic data for an ultra-light wing is a function of the fabric flexure, which in turn is directly related to angle of attack and airspeed.

There are range of other tests that could be performed with this wing model. Hopefully a structural failure test will not be one of them. Ideas for future experiments with this wing may include:

- 1) Building a rigid model of the ultra-light wing to provide base data so that a more accurate study of the effects of fabric flexure can be studied.
- 2) Re-doing the drag data and taking drag tare data.
- 3) Calculating the pitching moment about a more useful reference point such as 0.25c.
- 4) Performing this testing in a different wind tunnel that can register the maximum forces endured by the wing.

Overall this was a very enjoyable project and it is encouraged that other students use this wing in individual or group testing--such as an AE 245 laboratory exercise.

Appendix A: Data Analysis

AE 592

SPECIAL PROJECT :

DATE : 12/16/88

1/5 SCALE ULTRA-LITE WING

FOR DR. H.W. SMITH

BY MIKE JAMES

TEMP = 73.8°F

P_{ATM} = 29.26 ↑P_S = TUBE # 39 = 39.49P_T = TUBE # 40 = 25.38TEST
NUMBER : 1

ZERO SCALE: ⊙ N

α	LIFT		DRAG		PITCHING MOMENT	
	S.F.	READING	S.F.	READING	S.F.	READING
99928 -12°	500	-33.3	1000	24.0	500	+ 34.5
99948 -10°	500	-25.5	500	38.5	200	- 21.0
99968 -8°	200	-27.5	500	29.0	500	- 38.0
99988 -6°	100	+29.0	500	20.8	1000	- 33.0
00008 -4°	500	+19.8	500	16.5	1000	- 47.0
00028 -2°	500	37.8	500	17.0	2000	- 30.0
00048 0°	1000	23.3	500	20.8	2000	- 35.3
00068 +2°	1000	30.5	500	30.8	2000	- 43.0
00088 +4°	1000	34.5	500	40.8	2000	-47.8
00108 +6°	1000	38.0	1000	22.2	2000	-51.5
00128 +8°	1000	40.0	1000	27.2	PEGGED ↓	
00148 +10°	1000	44.0	1000	32.0		
00168 +12°	1000	46.0	1000	39.0		
00188 +14°	1000	48.0	1000	46.0		
00208 +16°	1000	49.0	2000	23.5		
00228 +18°	1000	49.5	2000	30.2		
00248 +20°	1000	51.0	2000	36.0		

AE 592

SPECIAL PROJECT :

DATE : 12/16/88

1/5 SCALE ULTRA-LITE WING

FOR DR. H.W. SMITH

BY MIKE JAMES

TEMP = 73.8°F

P_{ATM} = 29.26P_S = TUBE # 39 = 23.50P_T = TUBE # 40 = 25.12TEST
NUMBER : 2ZERO SCALE: ⊙ N
CALIBRATED TO 500

α	LIFT		DRAG		PITCHING MOMENT	
	S.F.	READING	S.F.	READING	S.F.	READING
00248 +20°	1000	33.0	2000	20.8	2000	-50.0
+18°	1000	31.5	1000	44.5	2000	-49.0
+16°	1000	31.8	1000	33.0	2000	-45.0
+14°	1000	30.8	1000	27.5	2000	-40.0
+12°	1000	29.5	1000	23.3	2000	-38.5
+10°	1000	27.8	1000	19.0	2000	-37.5
+8°	1000	26.0	500	39.8	2000	-36.3
+6°	1000	25.5	500	32.0	2000	-35.0
+4°	1000	22.8	500	24.3	2000	-32.3
+2°	500	48.0	500	17.5	2000	-28.7
0°	500	36.0	200	43.5	1000	-38.5
-2°	500	23.3	200	39.8	1000	-32.8
-4°	200	39.5	200	40.0	1000	-23.0
-6°	100	34.0	200	46.0	500	-38.5
-8°	50	-28.5	500	20.3	200	-35.0
-10°	200	-34.0	500	28.8	50	+38.0
-12°	200	-47.5	500	40.0	500	+27.5

AE 592

SPECIAL PROJECT :

DATE : 12/16/88

1/5 SCALE ULTRA-LITE WING

@ 2300

FOR DR. H. W. SMITH

TEMP = 76.0

BY MIKE JAMES

P_{ATM} = 29.27P_S = TUBE # 39 = 30.82P_T = TUBE # 40 = 25.59TEST
NUMBER : 3ZERO SCALE: (Y) N
TO 1000

α	LIFT		DRAG		PITCHING MOMENT	
	S. F.	READING	S. F.	READING	S. F.	READING
+20°	2000	.320	2000	.50.0		
+18°	2000	.320	2000	.42.8		
+16°	2000	.320	2000	.34.0		
+14°	2000	.303	2000	.29.5		
+12°	2000	.298	2000	.25.5		
+10°	2000	.280	1000 2000	.50.0 .21.0		
+8°	2000	.253	1000 2000	.42.3 .15.3		
+6°	2000	.238	1000 2000	.35.0 .13.5		
+4°	2000	.215	1000 2000	.24.8 .9.5		
+2°	2000	.183	1000 2000	.20.0 .6.0		
0°	2000	.125	1000 2000	.14.5 .3.5		
-2°	2000	.070	1000 2000	.12.0 2.0		
-4°	2000	.010	1000 2000	.12.0 2.0		
-6°	2000	-.050	1000 2000	.16.0 4.0		
-8°	2000	-.085	1000 2000	.22.3 7.0		
-10°	2000	-.110	1000 2000	.29.5 10.5		
-12°	2000	-.125	1000 2000	.39.5 15.5		

LIFTING
STOPPED

BUFFER

AE 592

SPECIAL PROJECT :

 $\frac{1}{8}$ SCALE ULTRA-LITE WING

FOR DR. H. W. SMITH

BY MIKE JAMES

[SET TO MAX
PITCHING
MOMENT]

DATE : 12/16/38

② 2345

TEMP = 76.2° F

P_{ATM} = 29.30P_S = TUBE # 39 = 27.83P_T = TUBE # 40 = 25.19TEST
NUMBER : 4NOTE: APPARENT ERROR WHEN USING
MULTIPLE SCALE FACTORS :
WILL STICK TO 1 SCALE FACTOR.ZERO SCALE: (Y) N
TO 2000 α

LIFT

DRAG

PITCHING MOMENT

	S. F.	READING	S. F.	READING	S. F.	READING
+ 20°	2000	21.5	2000	32.9	2000	-50.0
+ 18°		20.3		27.0		-46.3
+ 16°		20.3		23.5		-43.0
+ 14°		20.0		18.5		-39.0
+ 12°		19.0		16.0		-37.3
+ 10°		18.0		13.8		-36.0
+ 8°		17.0		11.8		-35.0
+ 6°		16.3		9.5		-33.0
+ 4°		14.8		8.3		-30.0
+ 2°		13.0		5.3		-26.0
0°		10.0		3.8		-20.5
- 2°		6.2		3.3		-17.3
- 4°		2.8		3.3		-14.5
- 6°		0.2		4.0		-11.0
- 8°		-1.2		5.8		-5.8
- 10°		-4.0		8.0		-1.0
- 12°		-5.8		12.0		+ 8.5

AE 592

SPECIAL PROJECT :

DATE : 12/17/88

@ 0030

1/8 SCALE ULTRA-LITE WING

FOR DR. H. W. SMITH

TEMP = 76.2

BY MIKE JAMES

P_{ATM} = 29.30"P_S = TUBE # 39 = 33.58P_T = TUBE # 40 = 25.94TEST
NUMBER : 5ZERO SCALE: Y (N)
LAST SET ON 2000

α	LIFT		DRAG		PITCHING MOMENT	
	S. F.	READING	S. F.	READING	S. F.	READING
+12°	2000	45.0	2000	41.0		
+10°		43.0		34.5		
+8°		38.8		29.3		
+6°		35.8		24.3		
+4°		32.5		18.8		
+2°		29.0		14.8		
0°		21.3		11.0		
-2°		13.5		9.3		
-4°		6.2		9.0		
-6°		-1.5		12.0		
-8°		-5.5		16.0		
-10°		-8.3		20.0		
-12°		-10.3		26.5		

AE 592

SPECIAL PROJECT :

DATE : 12/17/88

1/5 SCALE ULTRA-LITE WING

@ 0050

FOR DR. H. W. SMITH

TEMP = 76.2

BY MIKE JAMES

*NOTE
RECORDED

#39 & #40

AT ZERO

ANGLE OF

ATTACK.

P_{ATM} = 29.30"P_S = TUBE # 39 = 36.78P_T = TUBE # 40 = 26.38TEST
NUMBER : 6ZERO SCALE: Y (N)
LAST ZEROED ON 2000 α

LIFT

DRAG

PITCHING MOMENT

	S. F.	READING	S. F.	READING	S. F.	READING
8°	2000	50.0	2000	38.8		
6°		46.5		32.2		
4°		42.3		26.0		
2°		36.5		20.8		
0°		28.3		16.3		
-2°		16.7		11.5		
-4°		6.0		13.9		
-6°		-3.3		18.0		
-8°		-11.3		25.8		

AE 592

SPECIAL PROJECT :

DATE : 12/17/38

DO :

- RECD OF MAX C_M
AT 2320

- SF. DRAG AT 1000

- C_M at 1000? $1/5$ SCALE ULTRA-LITE WING

FOR DR. H. W. SMITH

BY MIKE JAMES

② 0100

TEMP = 76.0

 P_{ATM} = 29.31 P_S = TUBE # 39 = 23.38 P_T = TUBE # 40 = 25.27TEST
NUMBER : 7

ZERO SCALE: ⊙ N

 α

LIFT

DRAG

PITCHING MOMENT

	S. F.	READING	S. F.	READING	S. F.	READING
+ 20°	2000	20.0	2000	31.8	2000	- 50.0
+ 18°		18.8		27.0		- 47.0
+ 16°		18.8		22.0		- 43.0
+ 14°		18.0		17.9		- 39.0
+ 12°		17.0		15.3		- 37.5
+ 10°		16.2		12.8		- 36.3
+ 8°		15.5		11.3		- 35.0
+ 6°		14.5		8.8		- 33.3
+ 4°		13.3		6.8		- 30.3
+ 2°		11.5		4.7		- 26.5
0°		8.5		3.4		- 21.0
- 2°		4.7		2.6		- 17.8
- 4°		1.5		1.6		- 14.9
- 6°		- 0.9		3.7		- 11.3
- 8°		- 1.5		5.4		- 6.6
- 10°		- 4.7		7.8		- 2.0
- 12°		- 6.1		10.9		+ 6.3

AE 592

SPECIAL PROJECT :

DATE : 12/17/99

1/5 SCALE ULTRA-LITE WING

@ 0130

FOR DR. H. W. SMITH

TEMP = 76.0

BY MIKE JAMES

P_{ATM} = 29.31P_S = TUBE # 39 = 26.58P_T = TUBE # 40 = 25.01TEST
NUMBER : 8ZERO SCALE: (Y) N
ZEROED TO 1000

α	LIFT		DRAG		PITCHING MOMENT	
	S. F.	READING	S. F.	READING	S. F.	READING
+20°	1000	20.5	1000	33.5	1000	-50.0
+18°		19.0		27.5		-45.5
+16°		19.0		24.0		-44.0
+14°		18.5		17.3		-35.5
+12°		18.0		14.5		-34.0
+10°		17.0		12.4		-33.0
+8°		16.8		10.0		-32.0
+6°		15.9		8.0		-30.0
+4°		14.0		5.7		-26.7
+2°		12.2		3.9		-21.8
0°		8.5		2.5		-17.5
-2°		5.7		2.5		-14.5
-4°		2.5		2.2		-12.2
-6°		-0.2		2.7		-9.7
-8°		-2.6		4.2		-5.5
-10°		-5.0		7.4		-1.0
-12°		-6.5		11.0		+8.0

Equations:

1. Lift Calculation: $L = \frac{(\text{Reading})(\text{Scale Factor})}{27}$

2. Drag Calculation $D = \frac{(\text{Reading})(\text{Scale Factor})}{100}$

3. Pitching Moment Calculation: $PM = \frac{(\text{Reading})(\text{Scale Factor})}{29 \times 12}$

4. Calculation of Tunnel Speed:

$$V = \sqrt{\frac{(P_T - P_S)(3.2174)}{\rho}} \quad ; \quad \rho = \frac{P}{1716 T}$$

5. Calculation of Reynold's Number:

$$R_N = \frac{\rho V \bar{c}}{\mu} \quad ; \quad \mu = 3.408 \times 10^{-7} + 5.48 \times 10^{-10} T (^{\circ}F)$$

6. Calculation of C_L :

$$C_L = \frac{L}{\bar{q} S} \quad ; \quad \bar{q} = \frac{1}{2} \rho V^2$$

7. Calculation of C_D :

$$C_D = \frac{D}{\bar{q} S}$$

8. Calculation of C_M :

$$C_M = \frac{PM}{\bar{q} S \bar{c}}$$

```

10 RHO=0
20 L=0
30 D=0
40 TEMP=0
50 PRESS=0
60 PM=0
70 MU=0
80 V=0
90 CDTARE = 0
100 INPUT "TRIAL RUN NUMBER =";NUM
110 INPUT "STATIC PRESSURE =";PS
120 INPUT "TOTAL PRESSURE =";PT
130 INPUT "PRESSURE IN INCHES HG =";P
140 INPUT "TEMPERATURE IN DEGREES FARENHEIT =";T
150 INPUT "WING CHORD IN FEET =";C
160 INPUT "WING SPAN IN FEET =";B
170 S = B*C
175 PRINT "WING AREA =";S
180 PRESS = P*70.722
185 PRINT "PRESSURE =";PRESS
188 PRINT "PRESSURE ="PRESS
190 TEMP = T+459.6
195 PRINT "TEMPERATURE =";TEMP
200 RHO = PRESS/(1716*TEMP)
210 V = ((PS-PT)*3.2174/RHO)^.5
220 Q = .5*RHO*(V^2)
225 PRINT "DYNAMIC PRESSURE =";Q
230 MU = ((5.48*10^-10)*T)+(3.408*10^-7)
235 PRINT "VISCOSITY =";MU
240 RN = RHO*V*C/MU
250 LPRINT "WIND TUNNEL RUN NUMBER ";NUM
260 LPRINT "TUNNEL VELOCITY IN FT/S =";V
270 LPRINT "REYNOLDS NUMBER =";RN
280 LPRINT "      ALPHA      CL      CD      CM      "
290 LPRINT "-----"
300 INPUT "SCALE FACTOR =";SF
305 INPUT "ANGLE OF ATTACK =";ALPHA
310 INPUT "LIFT READING =";LREAD
320 L = LREAD*SF/27
330 CL = L/(Q*S)
340 INPUT "DRAG READING =";DREAD
350 D = DREAD*SF/100
360 CD = (D/(Q*S))-CDTARE
370 INPUT "PITCHING MOMENT READING =";PMREAD
380 PM = PMREAD*SF/348
390 CM = PM/(Q*S*C)
400 LPRINT TAB(4) ALPHA TAB(15) CL TAB(30) CD TAB(47) CM
410 GOTO 305

```

WIND TUNNEL RUN NUMBER 3

TUNNEL VELOCITY IN FT/S = 86.4358

REYNOLDS NUMBER = 432672.9

ALPHA	CL	CD	CM
20	1.410434	.5950268	0
18	1.410434	.5093429	0
16	1.410434	.4046182	0
14	1.335505	.3510658	0
12	1.313466	.3034637	0
10	1.234129	.2499112	0
8	1.115124	.1820782	0
6	1.04901	.1606572	0
4	.9476352	.1130551	0
2	.8065918	7.140321E-02	0
0	.5509507	4.165187E-02	0
-2	.3085324	2.380107E-02	0
-4	4.407606E-02	2.380107E-02	0
-6	-.2203803	4.760214E-02	0
-8	-.3746465	8.330375E-02	0
-10	-.4848367	.1249556	0
-12	-.5509507	.1844583	0

WIND TUNNEL RUN NUMBER 4

TUNNEL VELOCITY IN FT/S = 61.3908

REYNOLDS NUMBER = 307416.8

ALPHA	CL	CD	CM
20	1.877324	.7732828	-.3985074
18	1.772543	.6365438	-.3690178
16	1.772543	.5540288	-.3427163
14	1.746348	.4361504	-.3108358
12	1.65903	.3772112	-.2972865
10	1.571713	.3253446	-.2869253
8	1.484396	.2781932	-.2789551
6	1.423274	.2239691	-.2630149
4	1.292298	.1956783	-.2391044
2	1.135126	.1249512	-.2072238
0	.8731739	8.958764E-02	-.163388
-2	.5413678	.0777998	-.1378836
-4	.2444887	.0777998	-.1155671
-6	1.746348E-02	9.430279E-02	-8.767162E-02
-8	-.1047809	.136739	-4.622686E-02
-10	-.3492696	.1886056	-7.970147E-03
-12	-.5064409	.2829084	6.774625E-02

WIND TUNNEL RUN NUMBER 5
 TUNNEL VELOCITY IN FT/S = 104.4355
 REYNOLDS NUMBER = 522964.7

ALPHA	CL	CD	CM
12	1.357762	.3340095	0
10	1.297417	.2810568	0
8	1.170693	.2386946	0
6	1.080175	.1979617	0
4	.9806059	.1531556	0
2	.8750022	.1205693	0
0 21.3	.6426741	.0896123	0
-2	.4073286	7.576313E-02	0
-4	.1870695	7.331915E-02	0
-6	-4.525874E-02	9.775888E-02	0
-8	-.1659487	.1303452	0
-10	-.3107767	.2158842	0
-10	-.2504317	.1629315	0
-12	-.3107767	.2158842	0

WIND TUNNEL RUN NUMBER 6
 TUNNEL VELOCITY IN FT/S = 121.8479
 REYNOLDS NUMBER = 610158.1

ALPHA	CL	CD	CM
8	1.108258	.2322023	0
6	1.03068	.192704	0
4	.9375865	.1555995	0
2	.8090285	.1244796	0
0	.6272741	9.754889E-02	0
-2	.3701582	6.882284E-02	0
-4	.132991	8.318586E-02	0
-4	.132991	8.318586E-02	0
-6	-7.314504E-02	.1077227	0
-8	-.2504664	.1544025	0

WIND TUNNEL RUN NUMBER 7

TUNNEL VELOCITY IN FT/S = 66.60797

REYNOLDS NUMBER = 333876

ALPHA	CL	CD	CM
20	1.482431	.6364076	-.3382829
18	1.393485	.5403461	-.3179859
16	1.393485	.440282	-.2909233
14	1.334188	.3582294	-.2638607
12	1.260066	.3061961	-.2537122
10	1.200769	.2561641	-.2455934
8	1.148884	.2261448	-.236798
6	1.074763	.1761128	-.2252964
4	.9858166	.1360872	-.2049994
2	.8523978	9.406024E-02	-.17929
0	.6300331	6.804358E-02	-.1420788
-2	.3483713	5.203333E-02	-.1204287
-4	.1111823	0	-.1008083
-6	-.0667094	7.404743E-02	-7.645194E-02
-8	-.1111823	.1080692	-4.465334E-02
-10	-.3483713	.1561	-1.353132E-02
-12	-.4521415	.2181397	4.262365E-02

WIND TUNNEL RUN NUMBER 8

TUNNEL VELOCITY IN FT/S = 47.32559

REYNOLDS NUMBER = 237222.1

ALPHA	CL	CD	CM
20	1.504973	.6640236	-.3350507
18	1.394853	.545094	-.3048962
16	1.394853	.4757184	-.2948446
14	1.358147	.3429137	-.237886
12	1.32144	.2874132	-.2278345
10	1.248027	.2457879	-.2211335
8	1.233344	.198216	-.2144325
6	1.167272	.1585728	-.2010304
4	1.027787	.1129831	-.1789171
2	.8956426	7.730424E-02	-.1460821
0	.6240133	.049554	-.1172677
-2	.418456	.049554	-.0971647
-4	.1835333	4.360752E-02	-8.175237E-02
-6	-1.468267E-02	5.351832E-02	-.6499984
-8	-.1908747	8.325072E-02	-3.685558E-02
-10	-.3670667	.1466798	-6.701014E-03
-12	-.4771867	.2180376	5.360811E-02

V. STATIC TEST OF AN ULTRALIGHT AIRPLANE

Reprinted from *J. Aircraft*, Vol. 25, No. 1, January 1988

Howard W. Smith
Professor
Department of Aerospace Engineering
University of Kansas

Partially supported by
NASA Langley Research Center
Grant #NAG 1-345

Static Test of an Ultralight Airplane

Howard W. Smith*
University of Kansas, Lawrence, Kansas

This paper describes the work necessary to perform the static test of an ultralight airplane. A steel reaction gantry, loading whiffletrees, hydraulic actuation system, and instrumentation systems were designed. Load and stress analyses were performed on the airplane and on the newly designed gantry and whiffletrees. Load cell calibration and pressure indicator calibration procedures are described. A description of the strain and deflection measurement system is included. The engine, propeller, fuel, and pilot were removed and replaced with masses to fulfill center-of-gravity requirements prior to testing. Data obtained to date are compared to the analytical predictions.

Nomenclature

C_L	= wing lift coefficient
d	= displacement, mm
F_{cu}	= ultimate compression stress, ksi
h	= altitude, ft
M_x	= wing bending moment, N·m
n	= limit load factor
R_N	= nose wheel reaction, lb
R_L	= left main wheel reaction, lb
R_R	= right main wheel reaction, lb
S	= wing area, ft ²
V	= airplane speed, ft/s
W_0	= empty weight, lb
W_{BF}	= basic flight design weight, lb

Introduction

AS the service life of the fleet of ultralight vehicles increases, the number of fatal accidents is expected to increase as well. Several cases have been documented by the National Transportation Safety Board¹ in which the integrity of the structure was questioned. When similarities between cases occur, it is logical to formulate a plan to investigate the basic behavior of a typical vehicle.

The opportunity to formulate a plan presented itself in early 1985. Research on the aerodynamics and flight characteristics of an Airmass Sunburst "C" was drawing to a close and a master's thesis by Blacklock² was published. Consequently, a full-scale ultralight airplane was available for further research. A proposal was written and presented to the NASA Langley Research Center. The primary goal of this proposal was to perform a structural test to destruction of an ultralight airplane.

The structural floor and the ultralight airplane specimen are shown in Fig. 1. To perform a static test, a steel gantry and its sway bracing was designed.³ Similarly, the upper and lower whiffletrees were designed and integrated with the loading device. Finally, the strain and deflection systems were designed. This paper describes the details of the work accomplished.

Analysis

Design Criteria

In the early days, an airplane had to be able to carry the limit load without permanent deformation and the ultimate load for 3 s passing the static test sequence was a time of joy and celebration for the structures engineers. Nowadays, aircraft are governed by much more rigorous specifications. The static strength requirement has been retained, but is now only one element of a much larger array of specifications under a comprehensive umbrella known as the structural integrity program. Among the factors included are: corrosion, durability, damage tolerance, and flutter. Aircraft that are to be certified prior to use must meet or exceed specifications. These requirements are specified in either Federal Aviation Regulations or Military Specifications and the "meet or exceed" phrase is satisfied by analysis or by test or both.

A set of design guidelines for an ultralight has been published by the Powered Ultralight Manufacturers Association (PUMA).⁴ However, there are no specifications governing the structural integrity of an ultralight airplane. For this analysis, the ultralight was treated as though it were a normal category general aviation airplane governed by FAR-23. All related Mil-Specs and Mil-Standards were invoked as well.

It should be noted that student interest in this research project was very high. One student elected to write a report on a structural integrity program for ultralights,⁵ probably the only one of its kind in existence.

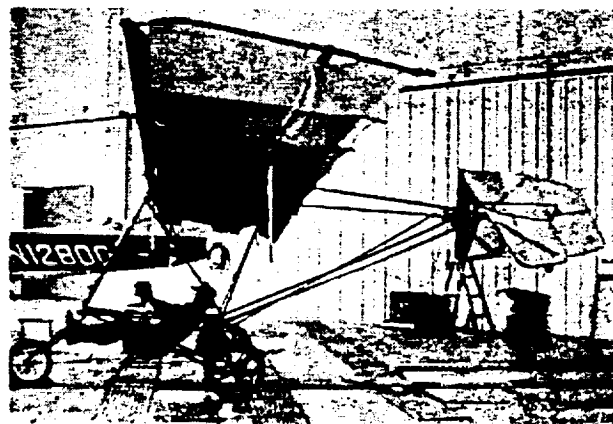


Fig. 1 Sunburst "C" ultralight.

Presented as Paper 86-2600 at the AIAA General Aviation Technology Meeting, Anaheim, CA, Sept. 29-Oct. 1, 1986; received Oct. 28, 1986; revision received June 12, 1987. Copyright © American Institute of Aeronautics and Astronautics, Inc., 1986. All rights reserved.

*Professor, Aerospace Engineering. Associate Fellow AIAA.

Table 1 Lift distribution

Speed (maneuvering)	69 ft/s
Altitude h	1000 ft
Weight W_{BF}	468 lb
C_L (max)	1.48
S	150.9 ft ²
n (limit)	3.8

Lift Distribution

Ordinarily, a structural test engineer begins with air load distributions as "known" values. Both spanwise and chordwise pressure distributions must be given beforehand to allow determination of "patch" loads. For this ultralight, six spanwise and two chordwise stations were selected to simulate the subsonic pressure distribution. In reality, the airfoil behavior is unknown, since it is only sail cloth stretched over the front and rear spar tubes. During a maximum positive load factor condition, the airfoil is taut and has a particular set of ordinates. During any other flight condition, including inverted flight, the ordinates are variable.

Since an air load distribution was not available, one was calculated using a quasivortex lattice method. This work was done by a student who favored this method and the analysis was performed with ease.^{6,7} With this knowledge, patch loads could be determined. Those data were incorporated in the upper whiffletree design. The design maneuvering speed at a limit load factor of 3.8 was 69.0 ft/s. (See Table 1.) The spanwise lift distribution is shown in Fig. 2. The spanwise drag distribution was assumed to be negligible.

Dead Weights

The weight breakdown for our test condition is given in Table 2. The engine, propeller, shaft, and mounts were removed and replaced with a mass whose magnitude and center of mass were correctly located. The lower whiffletree mass was included to correct the 1g dead weight loads. Fuel was replaced with water of the correct weight.

Our ultralight pilot, named Bellerophon, was constructed of army coveralls, worn-out army boots, a cap, and a mask (Halloween) for cosmetic purposes. The cap was adorned with a NASA logo. Bellerophon's center of gravity was built up with concrete cylinders at the buttock and thigh locations. The remainder was constituted from plastic bags and Kaw River sand. Weighing and loading him into the aircraft required the assistance of four strong students.

Overall airplane weight and center-of-gravity location was checked and rechecked by actual weighings with three balance scales under the wheels. Results of the weighings were: $R_N = 11.49$ lb, $R_L = 127.0$ lb, $R_R = 133.2$ lb, for a total of 271.69 lb. (See Fig. 3.)

Point Load Calculations

With many scientific developments, the creators of the breakthrough cannot foresee the eventual applications of their work. Likewise, Joseph Fourier could not have known that his work with sines and cosines would be used to calculate air load pressures on an ultralight airplane nor could Fred Whipple have known that his method would be used to approximate that air load.

The upper whiffletrees are simple three-point beam pairs made from ordinary 2×4 and 2×6 pieces of lumber. There are five "tiers" of trees. The first is the highest and the fifth the lowest. The trees are connected with heavy-duty turnbuckles. Tier 1 is connected to the steel gantry with a single steel strap. Tier 5 is just below the wing and is in direct contact with the tubular spars. Plywood bearing plates are used to spread the load along the spars. Tiers 1-3 are the spanwise trees, while tiers 4 and 5 assure the chordwise center-of-pressure location. With no load in the actuator, the ultralight is suspended above the hangar floor in straight and level flight.

Table 2 Weight breakdown of test aircraft, lb

Structure	
Tube WG-1	5.31
Wing skins	16.25
Landing gear	
Wheel-nose	3.12
Main wheels and tires	10.90
Rear axle	7.01
Seat	8.71
Powerplant	
Engine and propeller	78.38
Muffler	5.70
Propeller shaft	8.88
Misc., each < 3 lb	Remainder
W_0 Weight empty	277.48
Fuel	15.52
Pilot ("Bellerophon")	175.00
W_{BF} Basic flight weight	468.00

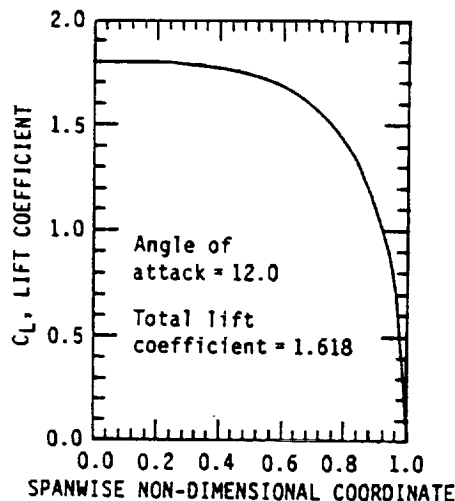


Fig. 2 Wing spanwise lift coefficient.

The upper whiffletree arrangement for the left-hand wing is shown in Fig. 4.

The lower whiffletree is a loading mechanism as well. A pair of steel straps connect at the engine mount holes and the U-straps bear directly on the fuselage cage tubes. These whiffletrees are commercial grade steel and are designated tiers 6 and 7. Tier 6 is adjacent to the fuselage and tier 7 (the lowest) connects to the 10,000 lb hydraulic actuator. A load cell is in series with the actuator. These linkages are bolted directly to a floor fitting where they are reacted. The floor fitting, called the "alligator," was specially designed for that purpose. It is located directly below the air load center-of-pressure vector P , shown in the lower whiffletree sketches (Figs. 5 and 6). All of the lower whiffletree members are made from standard AISC steel sections: rectangular tubing, tees, and flat straps.

Internal Loads Analysis

A stress analysis of the wing structure was performed using the air loads discussed above. Availability of the Polo finite-element method and its ease of use were the reasons for its selection.⁸ Results are given in DeAlmeida's report.⁵ The flying wire loads at the design limit load factor of $n = 3.8$ are:

Forward inboard 44 lb
Aft inboard 65 lb

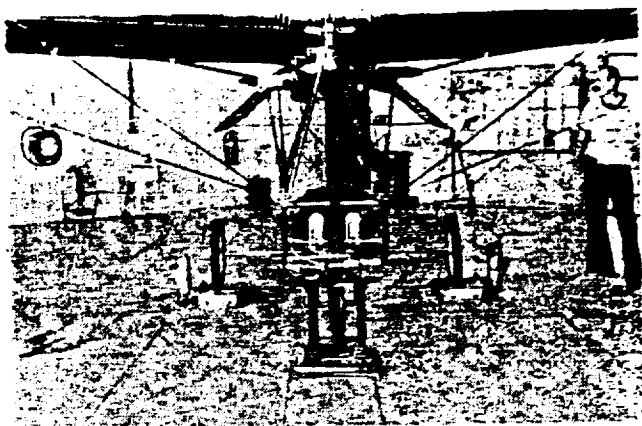


Fig. 3 Weight and center of gravity.

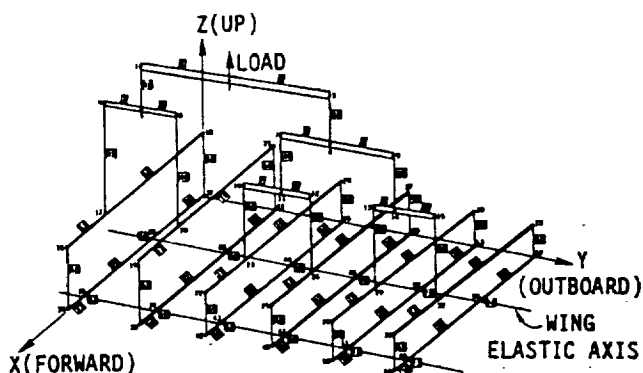


Fig. 4 Upper whiffletree.

Forward outboard 222 lb
Aft outboard 145 lb

Wing bending moments M_x and spar displacements d are shown in Figs. 7 and 8.

Systems Design

For this study, the test rig was divided into four independent systems. The design and assembly of each system is described below.

Hydraulic System

A 3000 psi hydraulic system was designed to apply the load. An Allis-Chalmers 10,000 lb, 8 in. stroke actuator and a Prince hand pump were purchased from a surplus machinery supplier. A pressure gage and short hydraulic lines were obtained from the same supplier. A schematic of the hydraulic system is shown in Fig. 9.

The Boeing Company supplied the hydraulic lines, a four-port Barksdale valve, and several hydraulic fittings. The 2 gal reservoir and hydraulic oil were purchased locally. These parts were assembled and the lines purged of air by two students. The system was tested during the two-by-four destruction test described below.

Load Cell System

A 5000 lb Baldwin-Lima-Hamilton load cell has been in the Aero Department for a number of years. A pair of load cell "eyes" had to be purchased to match the special internal threads. The eyes have 1 in. diameter self-aligning bearings. A pair of links connect to a smaller eye at each end. The smaller

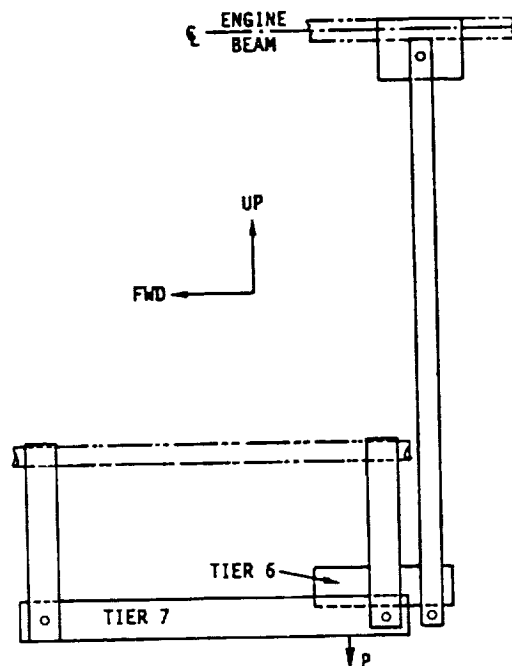


Fig. 5 Lower whiffletree, left side view.

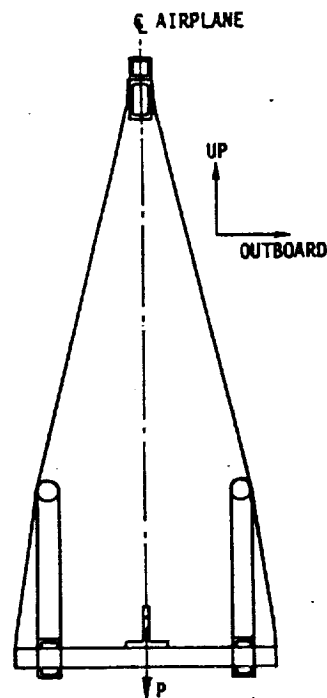


Fig. 6 Lower whiffletree, rear view.

eye shaft could then be gripped in test machine jaws. Excellent linearity was achieved. A calibration constant was determined to be 82 lb per unit readout.⁹

Deflection Measurement System

Large deflections were measured with a sliding scale system. In hazardous situations, a telescope or transit was used. This was the case when cable failures were imminent. When deflections were small (less than 1 in.), a dial indicator was used. Tip deflections of 3.70 in. limit were expected. The sliding scale concept was proved during the wood bending destruction test, which was recorded on video tape.

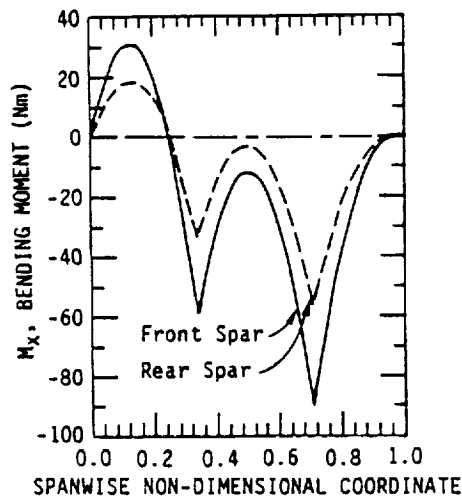


Fig. 7 Wing limit bending moments.

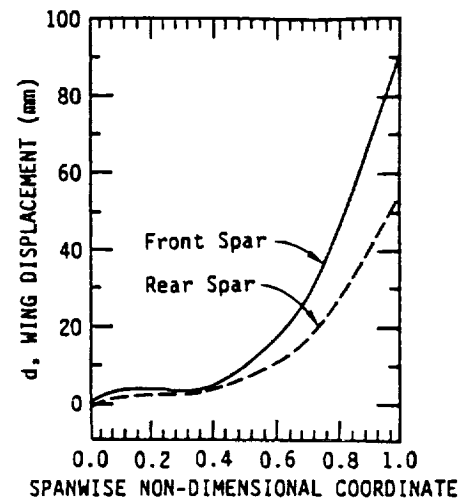


Fig. 8 Wing limit deflections.

Strain Measurements System

All strain gages were single-element foil gages from Micro Measurements. A 10 channel switch and balance unit and a strain readout unit were available from previous research. The strain gage terminal board was borrowed from the Aerospace Medical Research Laboratory. The resulting strain measurement system design was proved during the tube tension component tests described below. Data were taken with a Vishay-Ellis switch and balance unit and strain indicator.

Component Tests

Tube Compression

Compression tests of the 6061-T6 tubes were run to verify the heat treat level. The ultimate stress in compression was: F_{cu} (measured) = 47.8 ksi and F_{cu} (MIL-HDBK-5A) = 42.0 ksi.

Wood Bending

Wood bending tests were performed on a pair of medium-grade "S-P-F" lumber. The test simulated an upper whiffletree and was performed to spot check the modulus of rupture of "spruce-pine-fir," another unknown. Both the stress magnitude and the failure mode were missed. The modulus of rupture in bending, not to be confused with the civil engineering design value, was estimated to be 9600 psi. The wood beam ensemble failed in horizontal shear and "prying" near the point of maximum moment. The magnitude was 85% of the predicted ultimate load. For this test, the load-deflection curve was linear up to 50% of the failure load.

Cable Tension

Cable testing was very interesting and informative. Four assemblies of $\frac{1}{8}$ in. diameter, 7x19 aircraft cables were designed to represent the "flying wires" on the ultralight. They were fitted with thimbles, grommets, tangs, and Nico-press clamps. Failure load for the cable is estimated to be 1740 lb. None of the cables carried more than 975 lb. All "failed" by the cable sliding out of the Nico-press fitting. Cable testing is incomplete at this time. All cables will be fitted with double clamps and retested in an attempt to rupture the cable strands. Special safety precautions have been taken to keep humans out of a 100 in. cable whipping lethal radius drawn with each cable end as an arc center.

Recommendations

1) Unscathed portions of the ultralight, such as the wing tip, can be sawn off and used in future wind-tunnel work. The two-dimensional lift and drag coefficients should be obtained from minimum to maximum C_L .

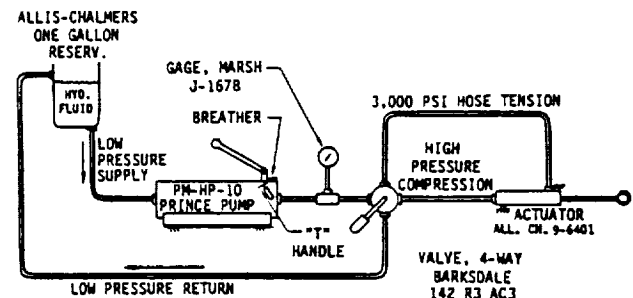


Fig. 9 Hydraulic system.

2) Almost nothing is known about the behavior of an ultralight structure under repeated loads. A durability and damage tolerance research program is highly recommended.

Acknowledgments

Many people freely volunteered to work on this project: Steve Waddell, Geoffrey Smith, Ron Schorr and Paul Oelschlaeger. Thanks to the Caroline Wire and Rope Company who supplied the cable and assembled the test specimens at no charge. This work was supported by NASA Langley Research Center under NASA Grant NAG 1-345 and the Aerospace Engineering Department of the University of Kansas.

References

- ¹"Safety Study: Ultralight Vehicle Accidents," National Transportation Safety Board, Rept. NTSB/SS-85/01, Feb. 7, 1985.
- ²Blacklock, C. L. Jr., "Summary of the General Powerplant, Weight and Balance and Aerodynamic Characteristics of an Ultralight Aircraft," M.S. Thesis, University of Kansas, Lawrence, Aug. 1984.
- ³Smith, H.W., "Design of Static Reaction Gantry for an Ultralight Airplane Destruction Test," AIAA Paper 85-4022, Oct. 14, 1985.
- ⁴"Airworthiness Standards for Powered Ultralight Vehicles," Powered Ultralight Manufacturers Association, Annandale, VA, Dec. 9, 1983.
- ⁵Turnipseed, Michael E., "Aircraft Structural Integrity Program for Ultralights," University of Kansas, Lawrence, May 7, 1986.
- ⁶DeAlmeida, S.F.M., "Aerodynamic and Structural Analyses of an Ultralight Aircraft," University of Kansas, Lawrence, May 6, 1986.
- ⁷Lan, C.T., "A Quasi Vortex Lattice Method in Thin Wing Theory," *Journal of Aircraft*, Vol. 11, 1974, p. 518.
- ⁸Lopez, L.A. et al., "Polo-Finite," University of Illinois, Urbana, 1985.
- ⁹Page, L., "Cable Testing for Ultralight Airplanes," University of Kansas, Lawrence, May 6, 1986.
- ¹⁰(All) Engineering Drawings, University of Kansas, Lawrence, (125 drawings total).